

Anatomy of torques from orbital Rashba textures: the case of Co/Al interfaces

A. Pezo,¹ N. Sebe,¹ A. Manchon,² V. Cros,¹ and H. Jaffrès¹

¹Laboratoire Albert Fert, CNRS, Thales, Université Paris-Saclay, 91767 Palaiseau, France

²Aix-Marseille Université, CNRS, CINaM, Marseille, France

(Dated: March 28, 2025)

In the context of orbitronics, the rising of the orbital angular momentum generated at light metal interfaces from orbital textures via orbital Rashba-Edelstein effects nowadays represent extraordinary alternatives to the usual heavy-metal spin-based materials. In the light of very recent experimental results [S. Krishnia *et al.*, *Nanoletters* 2023, 23, 6785], starting from state-of-the-art density functional theory simulations, we provide theoretical insights into the emergence of very strong orbital torques at the Co/Al interface location a strong orbital Rashba texture. By using linear response theory, we calculate the exerted orbital torque amplitudes, mainly of field-like intraband character, acting onto the ultrathin Co. Moreover, we show that an insertion of a single atomic plane of Pt between Co and Al is enough to suppress the effect which questions about the anatomy of the torque action clearly behaving differently than in the standard way. This work opens new routes to the engineering of spintronic devices.

Introduction - Orbital Hall (OHE) [1–3] and orbital Rashba-Edelstein effects (oREE) *via* the orbital angular momentum (OAM) [4–10] have recently emerged as new sources to knob quantum mechanical transport properties that can be potentially disrupting for the future generation of spintronic devices such orbital SOT-MRAM or spintronics THz emitters [11]. In a recent theoretical reference, Nikolaev *et al* [4] identified an orbital texture at the interface between the light metals Co and Al and they estimated the enhanced torques on Co resulting from the current-induced orbital Rashba-Edelstein polarization associated with the orbital texture, featuring thus possible novel torque functionalities. Moreover, the observation of long-range orbital generation of orbital accumulation at the surface like Ti [12] and Cr [13] by magneto-optical techniques have largely strengthened the interest for light metals (LM). Those phenomena appear as their spin counterparts, as the spin Hall (SHE) and spin Rashba-Edelstein effect (sREE), offering new mechanisms for data storage and energy-efficient electronics with the important difference lying on the dispensable role of spin-orbit interactions (SOI). SHE relying on heavy metals (HM) as Pt, W or Ta was already proven to realize efficient spin-orbit torque (SOT) functionalities [14–17]. The generation of a transversal orbital current resulting from an applied electric field (\mathcal{E}), *e.g.* via OHE, has garnered interest because it may interact with local moments over long-range distance [18, 19] thus enabling torques without any HM or even switch the magnetization with higher efficiency with the use of Nb, Ru and Cr LMs [20]. The demonstration of SOT in LM, such as Ti, has revealed the required properties to effectively achieve control of magnetization dynamics [21–24]. Additionally, the discovery of a large interfacial inverse oREE, along with recent terahertz (THz) emission using Ni [25–27] or CoPt alloys [28] as orbital sources, shows promise for uncovering new quantum properties in previously uncharted electronic devices.

From fundamentals viewpoint, oREE occurs when the

electric field \mathcal{E} induces a non-equilibrium orbital angular momentum (OAM) polarization in materials or at their interfaces lacking inversion symmetry. This feature appears as the counterpart of sREE generating a spin polarization via SOI in systems with broken inversion symmetry [29–32]. Nonetheless, it is generally admitted that the lack of coupling between OAM and magnetization represents a main difficulty to use them for manipulating a magnet. Still, oREE has the potential to convert OAM into spin and then interact with magnetic moments through SOI, possibly offering new efficient mechanisms for spintronic applications. Recent experiments [33] and theories [6, 8] have demonstrated orbital-charge conversion in oxide 2-dimensional electron gas, or with topological insulators [34]. It is anticipated that the latter conversion could be up to five or six times more efficient than the spin-to-charge conversion *e.g.* observed by terahertz spectroscopy [35]. Additionally, the generation of orbital photocurrents at BiAg₂ surfaces results in a significant orbital Rashba effect, presenting an excellent opportunity to manipulate electrical currents using the intrinsic orbital momentum of the light [36]. Furthermore, the large oREE in synthetic multiferroics accompanying its spin counterpart has been shown to produce substantial values capable of magnetization control [9].

In order to expand the range of materials able to offer spin manipulation, the orbital degree of freedom, ubiquitous in all electronic systems, has thus emerged as an attractive option. Nevertheless, spin and orbital degrees of freedom are intertwined, making it generally challenging to differentiate them. This complexity makes the use of low-Z materials essential [37] and the choice of the ferromagnet may have a significant quantitative impact on device improvement and design [38]. As recently demonstrated [10], and among different Co/LM structures, we presently conclusively demonstrate the existence of the orbital torque (OT) at Co/Al interfaces by means of joint Density Functional Theory (DFT) calculations with Kubo linear response theory; with

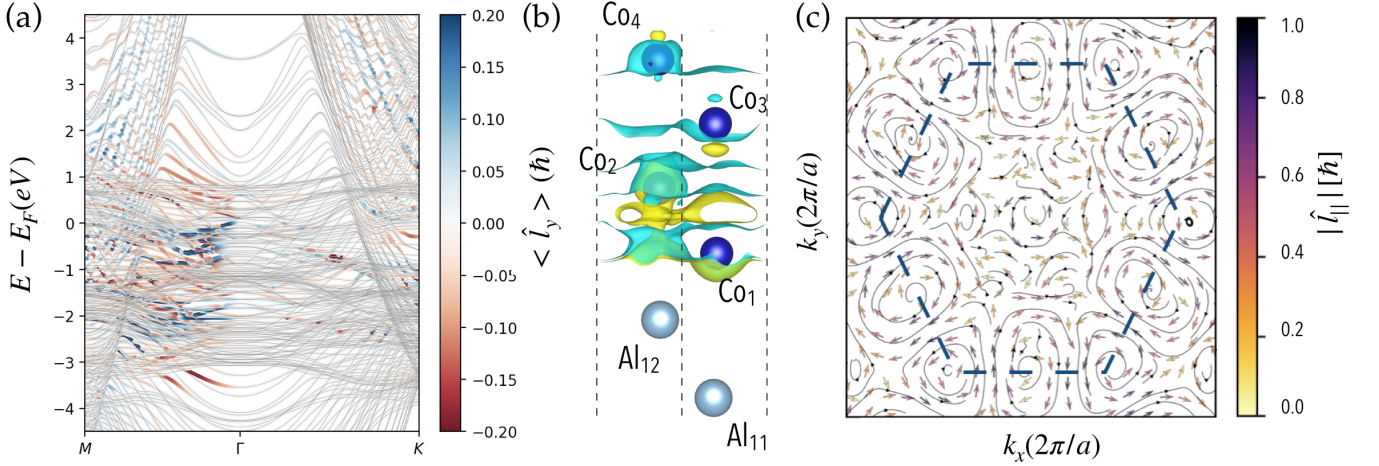


FIG. 1. (a) Electronic band structure along the high-symmetry path $M - \Gamma - K$ for the Co/Al bilayer showing the transverse orbital moment ($\langle \hat{l}_\perp \rangle = \langle \hat{l}_y \rangle$) projected at the Co(1) interfacial atoms displaying Rashba-like features. This is connected to the charge distribution shown in (b) where the charge difference resides at the interface between Co and Al layers. The orbital texture around the Brillouin zone which is the hexagonal shape represented by dashed lines is shown in (c).

the benefit here of avoiding orbital transport over long distance. By analyzing the corresponding interface properties largely explored [39] and subsequent electronic structure, it is concluded, in the present work, that the generated out-of-equilibrium orbital density exerts strong OT on an ultrathin Co magnet demonstrating thus that oREE represents the main contribution contrasting with the effect obtained by placing Pt, a reference SHE layer, sandwiched between Co and Al.

Co/Al interfaces - band structure - We have built a slab containing twelve layers of each fcc Al and hcp Co grown onto the same [111] directions [40] and with Co having the magnetization $\mathbf{M} = M_z$ pointing along the non-periodic direction \hat{z} normal to the layers. The in-plane lattice parameter was fixed at $a = 2.94 \text{ \AA}$ corresponding to energy minimization (Supp. Info. SI-I). By the use of self-consistent converged ground state, we obtained the electronic band structure of Co(12)/Al(12) projected onto the first Co(1) atomic plane in contact with Al(12) as displayed in Fig. 1(a). The emergent oREE is pictured by the mean value of the expected OAM values $\langle \hat{l}_y \rangle$ along different directions of the Brillouin zone, particularly exacerbated along $\bar{\Gamma} - \bar{M}$. This manifests the orbital texture displayed on Fig. 1(c) as a result of the electrostatic field appearing at the Co/Al interface clearly visible in Fig. 1(b). We observe that the orbital texture, the two $\langle \hat{l}_{x,y} \rangle$ in-plane orbital components calculated onto the Fermi surface, as depicted in Fig. 1(c), manifests a chiral texture of large OAM amplitude reaching $0.6-0.8 \mu_B$ unlike the Co(12)/Cu(12) 'reference' interfaces showing no specific OAM feature (SI-II). The ensemble of these results describing the electronic band structure and OAM properties of Co/Al and Co/Cu systems are in both qualitative and quantitative agree-

ment with our previous work [4] for the same systems. This clearly demonstrates the power of the Wannierization method. Here, we propose complementary analyses by emphasizing on the orbital torque response related to our recent experiments [10].

In most cases the SOT exerted onto a ferromagnet within a HM/FM bilayer originate from two main sources: the spin/orbital Hall effect in the non-magnetic layer able to inject polarized electrons flowing normal to the HM/FM interface and giving rise to a net integrated spin torque along the $-\vec{M} \times (\vec{M} \times \delta\vec{s})$ direction, where \vec{m} is the unit vector of the magnet and $\delta\vec{s}$ points along the out-of-equilibrium spin orientation generated by the spin-current. This scenario is usually related to the Berry curvature emerging from the HM bulk band structure. The other contribution arises from spin/orbital accumulation generated by inversion symmetry breaking. It is inherently correlated to the interface between the FM and NM or HM as a response to an electric field parallel to the plane such that it mainly points out along $\vec{M} \times \delta\vec{s}$, giving rise to a local torque of field-like torque (FLT) component. The current-driven field component can be heuristically computed as $\vec{h}_i = (\Delta_{xc}/\mathcal{V}M_s)\delta\vec{s}_i$, with Δ_{xc} the *sp-d* exchange potential between itinerant (NM) and localized (FM) electrons, $\delta\vec{s}_i$ is the *i*-th Pauli spin matrix in regular cartesian coordinates, M_s is the saturation magnetization of the ferromagnet, \mathcal{V} is the volume of the unit cell. The out-of-equilibrium quantity $\delta\vec{s}_i$ is computed within the linear response formalism after quantum statistical averaging considering the symmetrized decomposition of Kubo-Bastin formula proposed in Ref. [41].

SOT is made possible via the SOI. However, at first glance the low-Z atoms constituting Co/Al bilayers is not expected to contribute much. Nevertheless, recent

studies have pointed out the existence of large oREE in oxidized interfaces [42–46] and also at the interface between Co and metallic Al [4, 10] displaying unprecedented torques (FLT) with materials free of large SOI. We then conducted simulations of the SOT based on linear response theory. The full Hamiltonian can be decomposed into the kinetic part, \hat{H}_K , a SOI term, $\hat{H}_{SOC} = \xi_{SOC} (\hat{\nabla}V(r) \times \hat{p}) \cdot \hat{\sigma}$, small but not zero for a 3d magnet plus a magnetic or exchange part $\hat{H}_{xc} = -\mu_B \mathbf{B}_{xc} \cdot \hat{\sigma}$, where the exchange field \mathbf{B}_{xc} accounts for the difference between the effective Kohn-Sham potentials for minority and majority quasi-particles in Co. By applying \mathcal{E} , an out of equilibrium change in the magnetization $\delta\mathbf{M}$ enables the modification of the exchange following $\delta\mathbf{B}_{xc} = B_{xc}\delta\mathbf{M}/M$. Such a dynamical effect leads to a torque \mathcal{T} action onto \mathbf{M} within the unit cell given according to:

$$\mathcal{T} = \int d^3r \mathbf{M} \times \delta\mathbf{B}_{xc} = - \int d^3r \mathbf{B}_{xc} \times \delta\mathbf{M}. \quad (1)$$

As our approach is based on the linear response, the torque \mathcal{T} can be written in terms of the so-called torkance \mathbf{t} such that $\mathcal{T} = \mathbf{t}\mathcal{E}$ [47, 48]. The tensor \mathbf{t} can be decomposed into a respective *interband* and *intra-band* terms $\mathbf{t}_{ij} = \mathbf{t}_{ij}^{\text{Inter}} + \mathbf{t}_{ij}^{\text{Intra}}$, such that:

$$\mathbf{t}_{ij}^{\text{Inter}} = \frac{e\hbar}{2\pi\mathcal{N}} \sum_{\mathbf{k}, n \neq m} \frac{\text{Im} [\langle \psi_{\mathbf{k}n} | \hat{\mathcal{T}}_i | \psi_{\mathbf{k}m} \rangle \langle \psi_{\mathbf{k}m} | \hat{v}_j | \psi_{\mathbf{k}n} \rangle]}{(\varepsilon_m - \varepsilon_n)^2}$$

and

$$\mathbf{t}_{ij}^{\text{Intra}} = \frac{e\hbar}{\pi\Gamma\mathcal{N}} \sum_{\mathbf{k}, n} \text{Re} [\langle \psi_{\mathbf{k}n} | \hat{\mathcal{T}}_i | \psi_{\mathbf{k}n} \rangle \langle \psi_{\mathbf{k}n} | \hat{v}_j | \psi_{\mathbf{k}n} \rangle] \delta(\varepsilon_F - \varepsilon_n) \quad (2)$$

where we have adopted the clean limit case ($\Gamma \rightarrow 0$), but numerically is accounted for by a finite small value of the Fermi broadening energy $\Gamma = 0.075$ meV (throughout the paper). ε_F is the Fermi level, $\hat{\mathcal{T}}_i$ is the i -th component of the torque operator usually written as $\hat{\mathcal{T}} = \frac{-i}{\hbar} [\hat{\mathcal{H}}, \hat{\mathbf{s}}] = -\mu_B \hat{\sigma} \times \mathbf{B}_{xc}$ with v_j is the j -th component of the velocity operator. The exchange contribution to the Hamiltonian represents the main term owing in the case of a small SOI and is proportional to $\vec{\Omega}^{xc} = \Omega^{xc} \hat{m}$ and $\vec{\Omega}^{xc} = \frac{1}{2\mu_B} [V_{min}^{eff}(\vec{r}) - V_{maj}^{eff}(\vec{r})]$ is the exchange field. We took this part as the values of individual atomic magnetic moments after the self-consistent calculation. From symmetry arguments, the partition into *interband* and *intra-band* has to be assigned to mainly damping-like torque or DLT (\mathcal{T}_{xy}) and field-like torque or FLT (\mathcal{T}_{xx}) components respectively [18, 49] despite the lack of a mirror symmetry due to the hexagonal stacking may induce small mixing terms between FL and DL terms [4] (see also Table I comparing the orbital accumulation $\langle \hat{l}_y \rangle$ for respective *intra-band* vs. *interband* contributions).

Co/Al structures and orbital Rashba-Edelstein effects - We turn to the evaluation of both spin and orbital accumulation and related torkance response from the determination of the inverse Rashba-Edelstein χ_{xy}^{REE} tensors. We also considered the layer-resolved torkance of the Pt(10)/Co(3) SHE reference leading to same qualitative results than previous published works [50, 51]. We retained the *intra-band* term [7] according to:

$$\langle \hat{l}_y \rangle = -\frac{e\hbar}{4\pi} \int \partial_\epsilon f_\epsilon d\epsilon \text{Re Tr} \left\{ \hat{l}_y (G_0^R - G_0^A) \hat{v}_x (G_0^R - G_0^A) \right\} \mathcal{E}_x,$$

for \mathcal{E}_x along the \hat{x} direction and show the orbital accumulation projected on each layer of the structure as depicted in Fig. 2. For Co(12)/Al(12), the response profile $\chi_{xy}^{oREE} = \frac{\hbar \langle \hat{l}_y \rangle}{e\mathcal{E}_x a_0 \tau}$ displays a large peak of $\langle \hat{l}_y \rangle$ OAM density (in unit of $ea_0\tau\mathcal{E}$ with a_0 the Bohr radius and $\tau = (\frac{\hbar}{\Gamma})$ the momentum or spin relaxation time) at the Co(1) atoms interfacing Al (Fig. 2(a)). We find an orbital response from the oREE tensor χ_{xy}^{oREE} dominant by almost two orders of magnitude compared to the equivalent spin term (Fig. S9 SI-III). Moreover, $\langle \hat{l}_y \rangle$ is shown to be almost suppressed upon the inclusion of a very few number of Pt planes (Pt1, Pt2, Pt3) sandwiched between Co and Al (Fig. 2(e)). On adding Pt, we rather observe an oscillatory behavior of the generated OAM in Pt slightly propagating into neighboring Al layers (Fig. 2(b-d)). This feature may be understood as the spin-orbital imprint of the spin-polarization generated by sREE. Concerning Co(12)/Al(12), results are in very close agreement with Nikolaev et al. [4] using *Wannierization* techniques. The emergence of a very small spin-component (sREE) for Co/Al compared to the oREE counterpart (see table I) accounts for a strongly reduced out-of-equilibrium spin accumulation $\delta\hat{s}(\hat{l}) = \eta_{c-s(l)} \hat{z} \times \hat{j}_c$ unlike what is generally put forward for Rashba systems. This makes the strong peculiarity of such Co/Al system. We can give a fair estimate of the FLT component expected from oREE for Co/Al. Taking values for $\mathcal{E}_x \sim 2.5 \cdot 10^4$ V/m (equivalent to current density in Pt of $j_{Pt} = 10^{11}$ A/m²) the OAM reaches values as large as $\chi_{xy}^{oREE} \approx 5.94 \times 10^{-10} \hbar m/V/\text{atom}$ for which the effective FLT approaches $B_{FL} \approx \frac{\langle \xi_{SO} \rangle}{M_s t_F} \langle l_y \rangle = \frac{\langle \xi_{SO} \rangle}{M_s t_F} \chi_{xy}^{oREE} \mathcal{E} = 2.7$ mT in pretty good agreement with our experiments [45] and theory and calculation considering a slightly different lattice parameter [4]. We have calculated that χ_{xy}^{oREE} may vary vs. the in-plane lattice parameter (a) or strain but keeping substantial values over a large range of a (SI-III).

Torques at Co/Al interfaces: We have explicitly calculated both the FL and DL torque components considering respective *intra-band* t_{xx} (FLT) and *interband* t_{xy} (DLT) torkance. t_{xx} is shown in Fig. 3 for Co/Al as well as Co/Pt(1,2,3)/Al interfaces (see also Table I). For Co/Al, we have chosen the following setups, a) Al(12)/Co(12), b) Al(11)/Co(13) and c) Al(10)/Co(14) respectively and equivalent structures for Pt(1,2,3) insertion. The layer

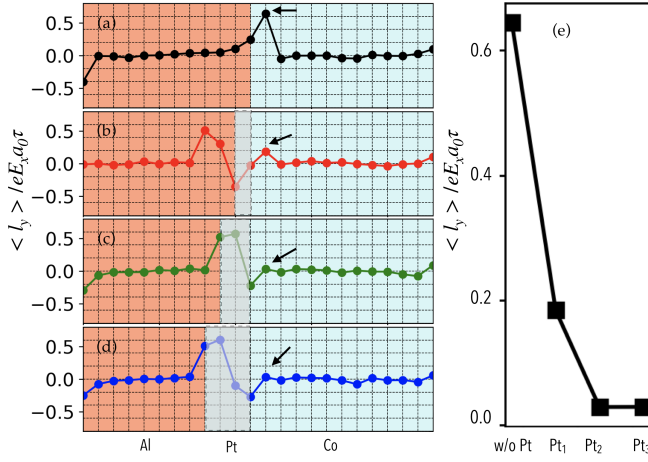


FIG. 2. oREE calculated for Co(12)/Al(12) bilayers for a value of broadening energy $\Gamma = 0.075$ eV (a) and with one (b), two (c) and three (d) Pt layers insertion. In (e) we show how the oREE on Co(1) signaled by black arrows from (a) to (d) decreases with the number of Pt layers.

projected torkance depicted in Fig. 3 (a,b,c) shows a gradual monotonous (non-oscillating) decaying behavior reaching its maximum at the interfacial Co(1) layer manifesting thus its strong orbital character [19]. On the Al side, although the orbital accumulation is not zero for Al(12) neighboring Co(1) (Fig. 2(a)), the torkance t_{xx} is calculated to be strictly zero because of the absence of any induced magnetic moment on Al(12) unlike the case of Pt (see table I). Moreover, from Ref. [49], the *intraband* torque t_{xx} is more related to the spin-current influx ($\langle Q^s \rangle^{\text{intra}}(r)$) according to $\langle T_{xc}^s \rangle(r)^{\text{intra}} = -\langle T_{SO}^1 \rangle(r)^{\text{intra}} + \nabla_r \langle Q^s \rangle^{\text{intra}}(r)$, both quantities to the right being linearly linked to the SOI strength (ξ_{SO}). We have indeed checked that *i*) the torkance t_{xx} disappears when the SOI is switched off in both Co and Al, *ii*) almost zero when SOI is absent in Co (only present in Al) or even absent only in Co(1) and *iii*) almost unaffected when SOI is only absent in Al in agreement with our expectations. Integrated torkance on the FM side is shown in Fig. 3(d) where a very large FLT (black) takes place in the Co/Al systems (almost constant for the three structures) and the much smaller ones (red) for equivalent structures with Pt1, Pt2 and Pt3 insertion. An integrated value of the torkance of $0.37 [ea_0]$ is equivalent to a field torque $B_{FL} = \left(\frac{e^* a_0}{M_s N} \right) t_{xx} \mathcal{E}$ (M_s is the atomic magnetic moment and N the number of Co atomic planes) giving thus $B_{FL} \approx 2$ mT (for $\mathcal{E} = 2.5 \times 10^4$ V/m or $j_s^{Pt} = 10^{11}$ A/m²).

The almost absence of oREE upon Pt insertion deserves some comments. It is experimentally demonstrated (unpublished) that inserting Pt leads to enhancement of the DL component (t_{xy}) while strongly reducing the FLT (t_{xx}). To access this information, we consider the Fermi sea (*interband*) component of the t_{xy} torkance derived

TABLE I. Co/Al and Co/Pt(1,2,3)/Al systems: $\langle \hat{l}_y \rangle$ -orbital (χ_i^{oREE}) and $\langle \hat{\sigma}_y \rangle$ -spin (χ_s^{sREE}) Rashba-Edelstein response at Co(1) interfacing Al or Pt. Values are given per atom. Integrated *intraband* t_{xx} (FL) and *interband* t_{xy} (DL) torkance components for Co/Al interfaces without/with Pt insertion.

Co/Al	$\chi_i^{\text{intra}} [10^{-10} \hbar m/V]$	$\chi_i^{\text{inter}} [10^{-10} \hbar m/V]$	$t_{xx} [ea_0]$
w/o Pt	5.94	0.20	0.37
1 Pt	1.56	0.18	-0.08
2 Pt	0.52	0.22	0.10
3 Pt	0.44	0.16	0.15
	$\chi_s^{\text{intra}} [10^{-10} \hbar m/V]$	$\chi_s^{\text{inter}} [10^{-10} \hbar m/V]$	$t_{xy} [ea_0]$
w/o Pt	0.12	-0.002	-0.04
1 Pt	-0.3	-0.01	0.33
2 Pt	-0.42	-0.14	-0.08
3 Pt	-0.50	0.02	0.13

from the Kubo formula (table I SI-IV). Those are displayed in Fig. 4, where t_{xy} is layer projected for the case of Pt1(a), Pt2(b) and Pt3(c). We demonstrate quite large values for the DLT with integrated value of the t_{xy} torkance depicted in Fig. 4(d) of the same order of magnitude than t_{xx} previously discussed. Moreover, a clear oscillating character from plane to plane of the DLT (as for FLT) in the case of Pt insertion exhibits the exchange interactions between spin and local moment mainly arising from either spin-Hall effect (SHE) or sREE from Pt layer(s) [19]. We recover the SOT magnitude obtained on reference Co(3)/Pt(10) (SI-IV) samples together with a characteristic oscillating behavior are in close agreement with Refs. [47, 48].

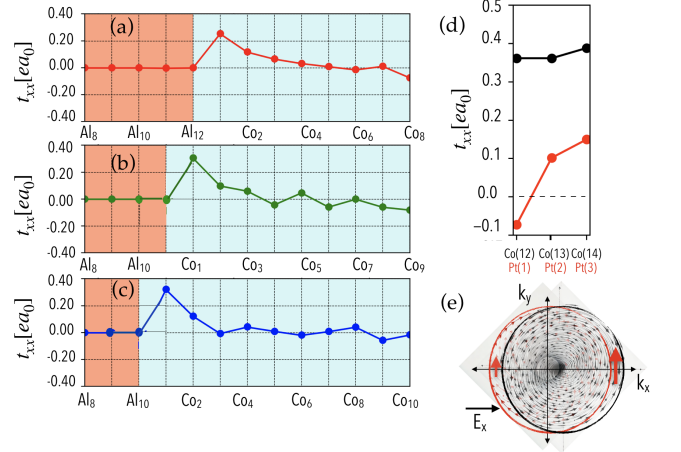


FIG. 3. Torkance components t_{xx} (mainly FLT) in units ea_0 calculated for Co/Al bilayers with increasing numbers of FM layers, namely, (a) corresponds to the t_{xx} for Al(12)/Co(12) bilayers, (b) Al(11)/Co(13) and (c) Al(10)/Co(14) bilayers respectively. In (d) we show the integrated value of t_{xx} over four layers within the FM side which arises from the OREE schematically depicted in (e).

Coming back to Co(12)/Al(12), t_{xy} values (DLT) remain

small (Fig. 4(d)) indicating that both *interband* orbital and spin torques contribute much less than their *intra-band* orbital counterpart (FLT). This emphasizes the strong local character of the orbital accumulation on Co(1) plane preventing thus any momentum precession inside Co. This is made possible by the confinement experienced by the interfacial evanescent states. The relationship between the OAM generated by oREE and the electronic escape time into the bulk Co states has been discussed in a previous work [52].

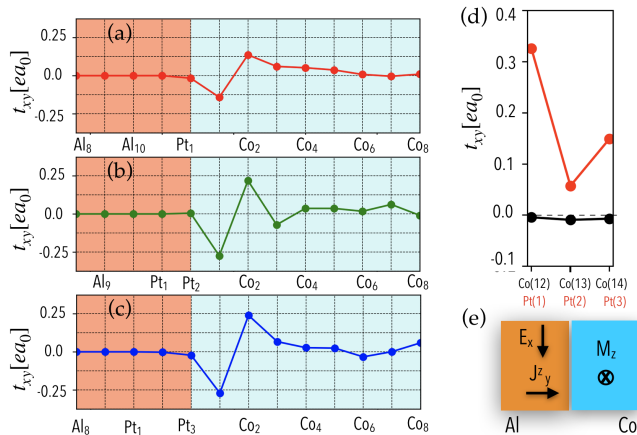


FIG. 4. t_{xy} [ea_0] torque (DLT) calculated for Al/Pt(1,2,3)/Co. (a) t_{xy} for Al(11)/Pt(1)/Co(12) bilayers, (b) Al(10)/Pt(2)/Co(12) and (c) Al(9)/Pt(3)/Co(14) bilayers respectively. (d) Integrated value of t_{xy} over four layers within the FM side arising from the SHE schematically depicted in (e). Results for Co/Al in (d) showcasing almost no DLT (black).

Discussion - Our simulations reveal a significant difference between Co/Al and other type of interfaces (as for Co/Cu taken as a reference [10]). The Mulliken charge analysis indicates a nearly order-of-magnitude difference

between the two systems, which accounts for the pronounced oREE observed at the Co/Al interface (SI-V). In comparison, the introduction of Pt resulted in a smaller Mulliken charge value relative to the Co/Al interface, underscoring the importance of chemical bonding among the atomic constituents. Furthermore, as listed in the SI and for direct comparison, we also have considered Co/Ti, Co/Mg interfaces giving negligible values for the OAM polarization as well as both FLT and DLT demonstrating thus the very specificity of Co/Al systems among other possible LM to observe oREE phenomenon.

To conclude, we have calculated the SOT for each odd and even orbital torque component, showing that our calculations based on the Kubo formalism ruled out the presence of a damping-like contribution for Co/Al. The observed decay on inserting Pt atomic planes, of mainly SHE character, aligns with the decreasing FL component, thereby validating our simulations. These results are significant because they enable us to study the anatomy of the oREE in the absence of a spin counterpart, which could guide the development of future spintronics devices with low-Z components.

ACKNOWLEDGMENTS

The authors thank Albert Fert, Nicolas Reyren and S. Nikolaev (Univ. Osaka, Japan) for fruitful discussions. This study has been supported by the French National Research Agency under the project ANR-20-CE30-0022-02 'ORION', by the project ANR-22-CE30-0026 'DYNTOP', by a France 2030 government grant managed by the French National Research Agency PEPR SPIN ANR-22-EXSP0009 (SPINTHEORY) and by the EIC Pathfinder OPEN grant 101129641 'OBELIX'. N. Sebe benefits from a France 2030 government grant managed by the French National Research Agency (ANR-22-PEPR-0009 Electronique-EMCOM).

-
- [1] Dongwook Go, Daegeun Jo, Changyoung Kim, and Hyun-Woo Lee, "Intrinsic spin and orbital hall effects from orbital texture," *Phys. Rev. Lett.* **121**, 086602 (2018).
 - [2] Armando Pezo, Diego García Ovalle, and Aurélien Manchon, "Orbital hall effect in crystals: Interatomic versus intra-atomic contributions," *Phys. Rev. B* **106**, 104414 (2022).
 - [3] Leandro Salemi and Peter M. Oppeneer, "First-principles theory of intrinsic spin and orbital hall and nernst effects in metallic monoatomic crystals," *Phys. Rev. Mater.* **6**, 095001 (2022).
 - [4] Sergey A. Nikolaev, Mairbek Chshiev, Fatima Ibrahim, Sachin Krishnia, Nicolas Sebe, Jean-Marie George, Vincent Cros, Henri Jaffrès, and Albert Fert, "Large chiral orbital texture and orbital edelstein effect in co/al heterostructure," *Nano Letters* **24**, 13465–13472 (2024).
 - [5] Dongwook Go, Daegeun Jo, Tenghua Gao, Kazuya Ando, Stefan Blügel, Hyun-Woo Lee, and Yuriy Mokrousov, "Orbital rashba effect in a surface-oxidized cu film," *Phys. Rev. B* **103**, L121113 (2021).
 - [6] Annika Johansson, Börge Göbel, Jürgen Henk, Manuel Bibes, and Ingrid Mertig, "Spin and orbital edelstein effects in a two-dimensional electron gas: Theory and application to strtio₃ interfaces," *Phys. Rev. Res.* **3**, 013275 (2021).
 - [7] Leandro Salemi, Marco Berritta, and Peter M. Oppeneer, "Quantitative comparison of electrically induced spin and orbital polarizations in heavy-metal/3d-metal bilayers," *Phys. Rev. Mater.* **5**, 074407 (2021).
 - [8] Annika Johansson, "Theory of spin and orbital edelstein effects," *Journal of Physics: Condensed Matter* **36**, 423002 (2024).
 - [9] Armando Pezo, Andrés Saul, Aurélien Manchon, and

- Rémi Arras, “Spin and orbital rashba effects at the ni/hfo₂ interface,” (2024), [arXiv:2412.04927](https://arxiv.org/abs/2412.04927) [cond-mat.mtrl-sci].
- [10] Sachin Krishnia, Yanis Sassi, Fernando Ajejas, Nicolas Sebe, Nicolas Reyren, Sophie Collin, Thibaud Denneulin, András Kovács, Rafal E. Dunin-Borkowski, Albert Fert, Jean-Marie George, Vincent Cros, and Henri Jaffrès, “Large interfacial rashba interaction generating strong spin-orbit torques in atomically thin metallic heterostructures,” *Nano Letters* **23**, 6785–6791 (2023).
 - [11] Qiming Shao, Peng Li, Luqiao Liu, Hyunsoo Yang, Shunsuke Fukami, Armin Razavi, Hao Wu, Kang Wang, Frank Freimuth, Yuriy Mokrousov, Mark D. Stiles, Satoru Emori, Axel Hoffmann, Johan Åkerman, Kaushik Roy, Jian-Ping Wang, See-Hun Yang, Kevin Garello, and Wei Zhang, “Roadmap of spin-orbit torques,” *IEEE Transactions on Magnetics* **57**, 1–39 (2021).
 - [12] Young-Gwan Choi, Daeyeun Jo, Kyung-Hun Ko, Dongwook Go, Kyung-Han Kim, Hee Gyum Park, Changyong Kim, Byoung-Chul Min, Gyung-Min Choi, and Hyun-Woo Lee, “Observation of the orbital hall effect in a light metal ti,” *Nature* **619**, 52–56 (2023).
 - [13] Igor Lyalin, Sanaz Alikhah, Marco Berritta, Peter M. Oppeneer, and Roland K. Kawakami, “Magneto-optical detection of the orbital hall effect in chromium,” *Phys. Rev. Lett.* **131**, 156702 (2023).
 - [14] J. E. Hirsch, “Spin hall effect,” *Phys. Rev. Lett.* **83**, 1834–1837 (1999).
 - [15] Jairo Sinova, Sergio O. Valenzuela, J. Wunderlich, C. H. Back, and T. Jungwirth, “Spin hall effects,” *Rev. Mod. Phys.* **87**, 1213–1260 (2015).
 - [16] Luqiao Liu, Takahiro Moriyama, D. C. Ralph, and R. A. Buhrman, “Spin-torque ferromagnetic resonance induced by the spin hall effect,” *Phys. Rev. Lett.* **106**, 036601 (2011).
 - [17] Luqiao Liu, Chi-Feng Pai, Y. Li, H. W. Tseng, D. C. Ralph, and R. A. Buhrman, “Spin-torque switching with the giant spin hall effect of tantalum,” *Science* **336**, 555–558 (2012), <https://www.science.org/doi/pdf/10.1126/science.1218197>.
 - [18] Hiroki Hayashi, Daeyeun Jo, Dongwook Go, Tenghua Gao, Satoshi Haku, Yuriy Mokrousov, Hyun-Woo Lee, and Kazuya Ando, “Observation of long-range orbital transport and giant orbital torque,” *Communications Physics* **6**, 32 (2023).
 - [19] Dongwook Go, Daeyeun Jo, Kyoung-Whan Kim, Soogil Lee, Min-Gu Kang, Byong-Guk Park, Stefan Blügel, Hyun-Woo Lee, and Yuriy Mokrousov, “Long-range orbital torque by momentum-space hotspots,” *Phys. Rev. Lett.* **130**, 246701 (2023).
 - [20] Rahul Gupta, Chloé Bouard, Fabian Kammerbauer, J. Omar Ledesma-Martin, Arnab Bose, Iryna Kononenko, Sylvain Martin, Perrine Usé, Gerhard Jakob, Marc Drouard, and Mathias Kläui, “Harnessing orbital hall effect in spin-orbit torque mram,” *Nature Communications* **16**, 130 (2025).
 - [21] Dongwook Go, Jan-Philipp Hanke, Patrick M Buhl, Frank Freimuth, Gustav Bihlmayer, Hyun-Woo Lee, Yuriy Mokrousov, and Stefan Blügel, “Toward surface orbitronics: giant orbital magnetism from the orbital rashba effect at the surface of sp-metals,” *Scientific reports* **7**, 46742 (2017).
 - [22] Shilei Ding, Andrew Ross, Dongwook Go, Lorenzo Baldrati, Zengyao Ren, Frank Freimuth, Sven Becker, Fabian Kammerbauer, Jinbo Yang, Gerhard Jakob, Yuriy Mokrousov, and Mathias Kläui, “Harnessing orbital-to-spin conversion of interfacial orbital currents for efficient spin-orbit torques,” *Phys. Rev. Lett.* **125**, 177201 (2020).
 - [23] Dongwook Go, Daeyeun Jo, Tenghua Gao, Kazuya Ando, Stefan Blügel, Hyun-Woo Lee, and Yuriy Mokrousov, “Orbital rashba effect in a surface-oxidized cu film,” *Phys. Rev. B* **103**, L121113 (2021).
 - [24] Shilei Ding, Zhongyu Liang, Dongwook Go, Chao Yun, Mingzhu Xue, Zhou Liu, Sven Becker, Wenyun Yang, Honglin Du, Changsheng Wang, Yingchang Yang, Gerhard Jakob, Mathias Kläui, Yuriy Mokrousov, and Jinbo Yang, “Observation of the orbital rashba-edelstein magnetoresistance,” *Phys. Rev. Lett.* **128**, 067201 (2022).
 - [25] Tom S. Seifert, Dongwook Go, Hiroki Hayashi, Reza Rouzegar, Frank Freimuth, Kazuya Ando, Yuriy Mokrousov, and Tobias Kampfrath, “Time-domain observation of ballistic orbital-angular-momentum currents with giant relaxation length in tungsten,” *Nature Nanotechnology* **18**, 1132–1138 (2023).
 - [26] Yong Xu, Fan Zhang, Albert Fert, Henri-Yves Jaffres, Yongshan Liu, Renyou Xu, Yuhao Jiang, Houyi Cheng, and Weisheng Zhao, “Orbitronics: light-induced orbital currents in ni studied by terahertz emission experiments,” *Nature Communications* **15**, 2043 (2024).
 - [27] Renyou Xu, Xiaobai Ning, Houyi Cheng, Yuxuan Yao, Zejun Ren, Shaojie Liu, Mingcong Dai, Yong Xu, Sai Li, Ao Du, Xiaojun Wu, Fengxia Hu, Baogen Shen, Jirong Sun, Hui Zhang, and Weisheng Zhao, “Terahertz generation via the inverse orbital rashba-edelstein effect at the Ni/Cu_x interface,” *Phys. Rev. Res.* **7**, L012042 (2025).
 - [28] Yongshan Liu, Yong Xu, Albert Fert, Henri-Yves Jaffrès, Tianxiao Nie, Sylvain Eimer, Xiaoliang Zhang, and Weisheng Zhao, “Efficient orbitronic terahertz emission based on copt alloy,” *Advanced Materials* **36**, 2404174 (2024), <https://advanced.onlinelibrary.wiley.com/doi/pdf/10.1002/adma.202404174>.
 - [29] Yu. A. Bychkov and É. I. Rashba, “Properties of a 2D electron gas with lifted spectral degeneracy,” *Soviet Journal of Experimental and Theoretical Physics Letters* **39**, 78 (1984).
 - [30] V.M. Edelstein, “Spin polarization of conduction electrons induced by electric current in two-dimensional asymmetric electron systems,” *Solid State Communications* **73**, 233–235 (1990).
 - [31] Ioan Mihai Miron, Gilles Gaudin, Stéphane Auffret, Bernard Rodmacq, Alain Schuhl, Stefania Pizzini, Jan Vogel, and Pietro Gambardella, “Current-driven spin torque induced by the rashba effect in a ferromagnetic metal layer,” *Nature materials* **9**, 230–234 (2010).
 - [32] Aurelien Manchon, Hyun Cheol Koo, Junsaku Nitta, Sergey M Frolov, and Rembert A Duine, “New perspectives for rashba spin-orbit coupling,” *Nature materials* **14**, 871–882 (2015).
 - [33] Anas El Hamdi, Jean-Yves Chauleau, Margherita Boselli, Clémentine Thibault, Cosimo Gorini, Alexander Smogunov, Cyrille Barreteau, Stefano Gariglio, Jean-Marc Triscone, and Michel Viret, “Observation of the orbital inverse rashba-edelstein effect,” *Nature Physics* **19**, 1855–1860 (2023).
 - [34] Armando Pezo, Jean-Marie George, and Henri Jaffrès, “Theory of spin and orbital charge conversion at the sur-

- face states of $\text{bi}_{1-x}\text{sb}_x$ topological insulator,” *Phys. Rev. Res.* **6**, 043332 (2024).
- [35] E. Rongione, L. Baringthon, D. She, G. Patriarche, R. Lebrun, A. Lemaître, M. Morassi, N. Reyren, M. Mićica, J. Mangeney, J. Tignon, F. Bertran, S. Dhillon, P. Le Fèvre, H. Jaffrès, and J.-M. George, “Spin-momentum locking and ultrafast spin-charge conversion in ultrathin epitaxial $\text{bi}_{1-x}\text{sb}_x$ topological insulator,” *Advanced Science* **10** (2023), 10.1002/advs.202301124.
- [36] T. Adamantopoulos, M. Merte, D. Go, F. Freimuth, S. Blügel, and Y. Mokrousov, “Orbital rashba effect as a platform for robust orbital photocurrents,” *Phys. Rev. Lett.* **132**, 076901 (2024).
- [37] Dongwook Go and Hyun-Woo Lee, “Orbital torque: Torque generation by orbital current injection,” *Phys. Rev. Res.* **2**, 013177 (2020).
- [38] Junyeon Kim, Dongwook Go, Hanshen Tsai, Daegeun Jo, Kouta Kondou, Hyun-Woo Lee, and YoshiChika Otani, “Nontrivial torque generation by orbital angular momentum injection in ferromagnetic-metal/Cu/ al_2o_3 trilayers,” *Phys. Rev. B* **103**, L020407 (2021).
- [39] Sachin Krishnia, Libor Vojáček, Tristan Da Câmara Santa Clara Gomes, Nicolas Sebe, Fatima Ibrahim, Jing Li, Luis Moreno Vicente-Arche, Sophie Collin, Thibaud Denneulin, Rafal E. Dunin-Borkowski, Philippe Ohresser, Nicolas Jaouen, André Thiaville, Albert Fert, Henri Jaffrès, Mairbek Chshiev, Nicolas Reyren, and Vincent Cros, “Interfacial spin-orbitronic effects controlled with different oxidation levels at the co—al interface,” (2024), arXiv:2409.10685 [cond-mat.mtrl-sci].
- [40] Gauravkumar Patel, Fabian Ganss, Ruslan Salikhov, Sven Stienen, Lorenzo Fallarino, Rico Ehrler, Rodolfo A. Gallardo, Olav Hellwig, Kilian Lenz, and Jürgen Lindner, “Structural and magnetic properties of thin cobalt films with mixed hcp and fcc phases,” *Phys. Rev. B* **108**, 184429 (2023).
- [41] Varga Bonbien and Aurélien Manchon, “Symmetrized decomposition of the kubo-bastin formula,” *Phys. Rev. B* **102**, 085113 (2020).
- [42] Junyeon Kim, Dongwook Go, Hanshen Tsai, Daegeun Jo, Kouta Kondou, Hyun-Woo Lee, and YoshiChika Otani, “Nontrivial torque generation by orbital angular momentum injection in ferromagnetic-metal/Cu/ al_2o_3 trilayers,” *Phys. Rev. B* **103**, L020407 (2021).
- [43] Shilei Ding, Paul Noël, Gunasheel Kawthilyaa Krishnaswamy, and Pietro Gambardella, “Unidirectional orbital magnetoresistance in light-metal–ferromagnet bilayers,” *Phys. Rev. Res.* **4**, L032041 (2022).
- [44] Junyeon Kim, Jun Uzuhashi, Masafumi Horio, Tomoaki Senoo, Dongwook Go, Daegeun Jo, Toshihide Sumi, Tetsuya Wada, Iwao Matsuda, Tadakatsu Ohkubo, Seiji Mitani, Hyun-Woo Lee, and YoshiChika Otani, “Oxide layer dependent orbital torque efficiency in ferromagnet/cu/oxide heterostructures,” *Phys. Rev. Mater.* **7**, L111401 (2023).
- [45] S. Krishnia, B. Bony, E. Rongione, L. Moreno Vicente-Arche, T. Denneulin, A. Pezo, Y. Lu, R. E. Dunin-Borkowski, S. Collin, A. Fert, J.-M. George, N. Reyren, V. Cros, and H. Jaffrès, “Quantifying the large contribution from orbital rashba–edelstein effect to the effective damping-like torque on magnetization,” *APL Materials* **12** (2024), 10.1063/5.0198970.
- [46] B. Bony, S. Krishnia, Y. Xu, S. Collin, A. Fert, J. M. George, M. Viret, V. Cros, and H. Jaffrès, “Quantitative analysis of vectorial torques in thin 3d co ferromagnet using orbital-spin conversion,” (2025), arXiv:2501.09864 [cond-mat.mtrl-sci].
- [47] K. D. Belashchenko, Alexey A. Kovalev, and M. van Schilfgaarde, “First-principles calculation of spin-orbit torque in a co/pt bilayer,” *Phys. Rev. Mater.* **3**, 011401 (2019).
- [48] G. G. Baez Flores and K. D. Belashchenko, “Effect of interfacial intermixing on spin-orbit torque in co/pt bilayers,” *Phys. Rev. B* **105**, 054405 (2022).
- [49] Dongwook Go, Frank Freimuth, Jan-Philipp Hanke, Fei Xue, Olena Gomonay, Kyung-Jin Lee, Stefan Blügel, Paul M. Haney, Hyun-Woo Lee, and Yuriy Mokrousov, “Theory of current-induced angular momentum transfer dynamics in spin-orbit coupled systems,” *Phys. Rev. Res.* **2**, 033401 (2020).
- [50] G. G. Baez Flores and K. D. Belashchenko, “Effect of interfacial intermixing on spin-orbit torque in co/pt bilayers,” *Phys. Rev. B* **105**, 054405 (2022).
- [51] Frank Freimuth, Stefan Blügel, and Yuriy Mokrousov, “Spin-orbit torques in co/pt(111) and mn/w(001) magnetic bilayers from first principles,” *Phys. Rev. B* **90**, 174423 (2014).
- [52] J C Rojas Sánchez, L Vila, G Desfonds, S Gambarelli, J P Attané, J M De Teresa, C Magén, and A Fert, “Spin-to-charge conversion using rashba coupling at the interface between non-magnetic materials,” *Nature Communications* **4**, 2944 (2013).